THE JOURNAL OF BIOLOGICAL CHEMISTRY VOL. 285, NO. 20, pp. 15209–15219, May 14, 2010

Complementary Interactions of the Rod PDE6 Inhibitory Subunit with the Catalytic Subunits and Transducin*[S]

Received for publication, November 18, 2009, and in revised form, March 12, 2010 Published, JBC Papers in Press, March 15, 2010, DOI 10.1074/jbc.M109.086116

Lian-Wang Guo[‡1], **Abdol R. Hajipour**[‡§], **and Arnold E. Ruoho**[‡]

From the [‡]*Department of Pharmacology, University of Wisconsin School of Medicine and Public Health, Madison, Wisconsin 53706 and the* [§]*Pharmaceutical Laboratory, College of Chemistry, Isfahan University of Technology, Isfahan 84156, Iran*

Activation of the cyclic GMP phosphodiesterase (PDE6) by transducin is the central event of visual signal transduction. How the PDE6 inhibitory γ-subunit (Pγ) interacts with the catalytic subunits (Pαβ) and the transducin α-subunit (α_t) in this process is not entirely clear. Here we have investigated this issue, taking advantage of site-specific label transfer from throughout the full-length Pγ molecule to both α_t and Pαβ. The interaction profiling and pull-down experiments revealed that the Pγ C-terminal domain accounted for the major interaction with α_t bound with guanosine 5′-3-*O*-(thio)triphosphate (α_tGTPγS) in comparison with the central region, whereas an opposite pattern was observed for the Pγ-Pαβ interaction. This complementary feature was further exhibited when both α_tGTPγS and Pαβ were present and competing for Pγ interaction, with the Pγ C-terminal domain favoring α_t, whereas the central region demonstrated a preference for Pαβ. Furthermore, α_tGTPγS co-immunoprecipitated with PDE6 and *vice versa* in a Pγ-dependent manner. Either Pαβ or α_tGTPγS could be pulled down by the Btn-Pγ molecules on streptavidin beads that were saturated by the other partner, indicating simultaneous binding of these two partners to Pγ. These data together indicate that complementary Pγ interactions with its two targets facilitate the α_t·PDE6 "transducisome" formation. Thus, our study provides new insights into the molecular mechanisms of PDE6 activation.

The intricate visual transduction in rod photoreceptor cells provides a paradigm for G protein-coupled signaling. The outstanding visual sensitivity of the rod is largely due to the great signal amplification achieved by the cGMP[2] phosphodiesterase PDE6 (rod photoreceptor cGMP phosphodiesterase), the central effector enzyme (1). Upon absorption of a single photon, light-excited rhodopsin stimulates an exchange of GTP for GDP bound in the transducin α subunit (α_t) (2), which in turn relieves PDE6 from the inhibitory constraint exerted by its γ-subunit (Pγ). PDE6 activation causes rapid cGMP breakdown, which closes the cGMP-coupled ion channels, thus relaying visual signals to the brain in a form of electrical pulses (3). PDE6 in the rod is uniquely composed of a large catalytic heterodimer (Pαβ, ~100 kDa each subunit) to which bind two small identical Pγ subunits (~10 kDa) keeping the enzyme inactive in the dark (1, 4). The PDE6 structure is less well understood compared with the other key players in phototransduction. This is primarily due to the fact that solving the atomic structure of PDE6 has been hindered by the lack of an expression system to produce active Pαβ heterodimers in large amounts (5). A low resolution electron microscopy image of Pαβ has revealed a linear alignment of three distinct domains of each subunit: the tandem GAFa and GAFb domains on the N-terminal side that host non-catalytic cGMP binding and the C-terminal catalytic domain that performs cGMP hydrolysis (6). Direct allosteric communication between GAF domains and the catalytic domain has been recently reported (7).

The inhibitory Pγ subunit is an intrinsically disordered protein, yet structural elements important for its function are encoded in the free Pγ molecule (8). The Pγ sequence of 87 amino acids features a polycationic central domain (Gly^{19}–Gly^{49}) and a negatively charged C-terminal half that contains a linker region (Phe^{50}–Gly^{61}) and a hydrophobic C-terminal domain (Thr^{62}–Ile^{87}) (1, 9). The last C-terminal dozen or so residues (herein termed the inhibitory region) are involved in the interaction with the Pαβ catalytic domain (8, 10, 11). The very recently reported crystal structure of the chimeric PDE5/6 catalytic domain complexed with the Pγ(70–87) inhibitory peptide (5) has confirmed the previous suggestion that the highly hydrophobic C terminus ($Y^{84}GII^{87}$) directly blocks the cGMP entry into the catalytic pocket (12, 13). The other important Pαβ-interacting site on Pγ is the central domain, which has been shown to provide most of the binding strength for Pαβ (14). The central domain of Pγ binds to the Pαβ GAF domain (15, 16) and couples non-catalytic cGMP binding in a positively cooperative manner, thus regulating the PDE-inhibiting function of Pγ (14). Remarkably, the C-terminal domain and the central domain also constitute α_t-interacting sites (17–19).

An overlap of the Pγ C-terminal α_t-binding region (Thr^{62}–Ile^{87}) and the inhibitory region (Asn^{74}–Ile^{87}) forms the structural basis for transducin-mediated PDE6 activation (5, 8, 20). Various lines of evidence suggest that GTP-bound α_t activates PDE6 by physically displacing the inhibitory region of Pγ from

* This work was supported, in whole or in part, by National Institutes of Health Grant GM33138 (to A. E. R. and L.-W. G.).

[S] The on-line version of this article (available at http://www.jbc.org) contains supplemental Table S1 and Fig. S1.

[1] To whom correspondence should be addressed: Dept. of Pharmacology, University of Wisconsin School of Medicine and Public Health, 1300 University Ave., Madison, WI 53706. Tel.: 608-263-3980; Fax: 608-262-1257; E-mail: lianwangguo@wisc.edu.

[2] The abbreviations used are: cGMP, cyclic GMP; α_t, transducin α-subunit; Pαβ, PDE6 catalytic heterodimer; GAF, a domain derived from cGMP phosphodiesterases, adenylyl cyclases, and the *Escherichia coli* protein Fh1A; Pγ, PDE6 inhibitory subunit; GAP, GTPase-activating protein; ACTP, *N*-[3-iodo-4-azidophenylpropioamido-*S*-(2-thiopyridyl)]cysteine; mBP, 4-(*N*-maleimido)benzophenone; HPLC, high performance liquid chromatography; ROS, rod outer segment; DTT, dithiothreitol; BSA, bovine serum albumin; GTPγS, guanosine 5′-3-*O*-(thio)triphosphate.

the P$\alpha\beta$ catalytic pocket, thus initiating the signaling state of phototransduction (5, 8, 10–12, 20). In the ensuing transition state, α_tGTP is converted back to the GDP-bound inactive structure, which has lowered affinity with Pγ, thus releasing it to reinhibit PDE6 and terminate signaling (3). Fast visual recovery is ensured by great acceleration of the α_t GTPase activity, which is achieved by the GTPase-activating protein (GAP) complex composed of α_t, Pγ, RGS9-1 (the ninth member of the regulators of G-protein signaling in photoreceptors), and its constitutive partner Gβ5 as well as the membrane anchoring protein R9AP (3, 21). Much of the molecular details of the Pγ-α_tGTP interaction in the signaling state have been learned from the crystal structure of the partial transition state complex, which includes the GDP-AlF_4^--bound $\alpha_{t/i1}$ chimera, the half-Pγ (Gly^{46}–Ile^{87}), and the catalytic core of RGS9-1 (20). As visualized by this structure, a stretch of Pγ residues around Trp^{70} forms a tight interaction with α_t that is further reinforced by additional contacts provided by some residues in the Pγ inhibitory region. Recent NMR (8) and crystallography (5) studies indicated that when the Pγ inhibitory region was associated with the chimeric PDE5/6 catalytic domain, the critical α_t-binding residues Trp^{70} and Leu^{76}, however, were not involved. These studies lend further support to a model of PDE6 activation (5, 11); *i.e.* an engagement of α_tGTP with the Pγ residues Trp^{70} and Leu^{76} triggers a conformational change involving a hingelike rigid body movement of Pγ(78–87) away from the PDE6 catalytic pocket.

Thus, Pγ plays a pivotal role, not only for turning on but also for turning off phototransduction and keeping the signaling system inactive in the dark (9). Despite a wealth of information regarding phototransduction mechanisms, dynamic interactions of Pγ with α_t and P$\alpha\beta$, as well as RGS9-1, are not well understood. There has been controversy as to whether Pγ completely dissociates from P$\alpha\beta$ in the process of PDE6 activation. It is possible that whereas α_t sequesters the Pγ C-terminal region from the P$\alpha\beta$ catalytic domain, the central domain of Pγ stays bound to the P$\alpha\beta$ GAF domain until the binding is allosterically reduced by the dissociation of cGMP from the GAF domain (1). This scenario of simultaneous Pγ interactions with both α_t and P$\alpha\beta$ is consistent with the proposition of an intermediate α_t·PDE6 complex during PDE6 activation (17, 22–26). Earlier studies suggested that direct α_t-P$\alpha\beta$ contacts may be a driving force in forming the intermediate complex in the presence of disc membranes (24, 27). However, it has not been determined whether the Pγ interactions with α_t and P$\alpha\beta$ contribute important elements to the intermediate PDE6 activation complex.

As presented in this study, the label transfer approach, which has proven to be powerful for systematically detecting interactions of full-length molecules (16, 28, 29), offered us an opportunity to investigate this issue from a unique perspective. The data obtained through label transfer, immunoprecipitation, and pull-down suggest that complementary interactions, in which the Pγ C-terminal domain forms a strong interaction with α_t while the central region binds tightly with P$\alpha\beta$, assist the transducin·PDE6 complex formation, which elicits PDE6 activation.

EXPERIMENTAL PROCEDURES

The chemicals and reagents used in this study were from the sources described previously (16, 28) unless otherwise stated. The C-terminal Pγ peptide (Pγ(62–87)) was custom-synthesized at the Peptide Synthesis Facility of the Biotechnology Center, University of Wisconsin (Madison, WI).

Transducin Preparation—Using frozen dark-adapted bovine retinas (J. A. & W. L. Lawson Co.), rod outer segment (ROS) membranes were isolated, from which holotransducin was prepared as described previously (29, 30). α_tGDP and $\beta\gamma_t$ were then purified from holotransducin using a blue Sepharose CL-6B column. To prepare α_tGTPγS, GTPγS was added to ROS membranes, and α_tGTPγS was thus released and purified on the blue Sepharose CL-6B column. The purity of α_t was determined to be >95% by SDS-PAGE and Coomassie staining. The purified proteins were stored at −80 °C.

Preparation of PDE6—The samples of bovine PDE6 were kindly provided by Dr. Nikolai O. Artemyev at the University of Iowa and prepared according to established methods (4). Briefly, holo-PDE6 was extracted from bleached ROS membranes, and P$\alpha\beta$ was then obtained by removing Pγ through mild tryptic proteolysis of holo-PDE6. More vigorous tryptic treatment generated the P$\alpha\beta$ heterodimer with a nick at Lys^{146}/Lys^{147} on Pβ. It has been reported that nicked P$\alpha\beta$ has unaltered functional properties (12, 16). Unless otherwise stated, "P$\alpha\beta$" refers to nicked P$\alpha\beta$ throughout this paper. The P$\alpha\beta$ preparations were purified to >95% by a Mono-Q column (Amersham Biosciences), as judged from Coomassie-stained SDS gels.

Preparation of Pγ Photoprobes—The constructs for expressing the full-length wild type Pγ with the single cysteine at position 68 (29), and the single cysteine mutants were generated as described previously (28). They were expressed in *E. coli* and purified by chitin beads, followed by reversed-phase HPLC using the POROS 20 R2 resin (31). The truncated Pγ variants (29) with and without a His_6 tag at the N terminus (HisPγ(1–61) and Pγ(1–61), respectively) were prepared using the same protocol. Full-length Pγ (>95% pure) was used for preparation of Pγ photoprobes. The radioactive [^{125}I]ACTP-Pγ and nonradioactive [^{127}I]ACTP-Pγ photoprobes were prepared as described earlier (28).

The maleimido benzophenone (mBP)-Pγ photoprobes were prepared as described previously (16). Briefly, Pγ was derivatized with mBP in 10–20-fold molar excess, and mBP-Pγ was then separated from unreacted Pγ and free mBP through reversed phase HPLC. Correct molecular masses of the [^{127}I]ACTP-Pγ and mBP-Pγ photoprobes have been confirmed by electrospray ionization mass spectrometry conducted at the Chemistry Department Mass Spectrometry Facility of the University of Wisconsin (Madison, WI).

Functional Assay of the Pγ Photoprobes—The transducin GTPase activity assay was kindly conducted by Dr. Kirill A. Martemyanov (now at the University of Minnesota) and Dr. Vadim Y. Arshavsky (now at Duke University), using a single turnover technique as described previously (32). The assay was conducted at room temperature (22–24 °C) in a buffer containing 25 mM Tris-HCl (pH 8.0), 140 mM NaCl, and 8 mM $MgCl_2$.

The urea-treated ROS membranes, lacking endogenous activity of RGS9-1, were used as a source for the photoexcited rhodopsin required for transducin activation. The reactions were initiated by the addition of 10 μl of 0.6 μM [^{32}P]GTP (~10^5 dpm/sample) to 20 μl of urea-treated ROS membranes (20 μM final rhodopsin concentration) reconstituted with transducin heterotrimer (1 μM) and recombinant RGS9-1·Gβ5 complex (0.5 μM). The reactions were performed in either the absence or presence of Pγ derivatives (1 μM). The reaction was stopped by the addition of 100 μl of 6% perchloric acid. The ^{32}P formation was measured with activated charcoal. All assays were conducted in the absence of reducing agent due to the presence of the disulfide linkage between the photoreactive group and Pγ.

Photocross-linking/Label Transfer Using Pγ Photoprobes—A scheme is presented in supplemental Fig. S1*A* to explain the label transfer strategy. Unless otherwise described, photocross-linking reactions were performed in the HEPES buffer (10 mM HEPES, pH 7.5, 120 mM NaCl, 5 mM $MgCl_2$). Samples were contained in ultraclear polypropylene microcentrifuge tubes (Axygen). The reactions using [^{125}I]ACTP-Pγ photoprobes were exposed to the UV light generated by an AH-6 water-jacketed 1000-watt high pressure mercury lamp for 5 s at a distance of 10 cm (28). The reactions with mBP-Pγ were photolyzed at 5–10 °C for 2 × 15 min with a 5-min dark interval on ice in an RPR-100 Rayonet photochemical reactor equipped with 18 bulbs of 350 nm (Southern New England Ultraviolet Company). Immediately after photolysis, sample buffer was added to the reactions to final concentrations of 1% SDS and 50 mM DTT. The proteins were separated by SDS-PAGE and then subjected to Coomassie Blue staining and autoradiography. Autoradiography and protein quantitation were performed as described previously (28).

Pull-down Assays of Pγ Interactions with α_tGTPγS and P$\alpha\beta$ Using Affinity Beads—To immobilize the full-length Pγ to the streptavidin beads, biotinylated Pγ was prepared by covalently attaching maleimide-PEO_2-biotin (Pierce Biotechnology) to the single cysteine at position 3 of the Pγ mutant, L3C (28). The derivatization reaction and purification of the Btn-L3C derivative were performed following the protocol of mBP-Pγ preparation (16). To prepare Btn-Pγ(46–87), the Pγ 87C mutant was first derivatized with maleimide-PEO_2-biotin and then trypsinized, and Btn-Pγ(46–87) was purified by reversed phase HPLC using a C4 column (31).

For each pull-down reaction, 0.4 μl of Ultra-Link Plus immobilized streptavidin gel (Pierce) was first equilibrated with the pull-down buffer, which contains 20 mM HEPES, pH 7.5, 120 mM NaCl, 5 mM $MgCl_2$, 1 mM DTT, 0.1% *n*-dodecanoylsucrose (Calbiochem), and 50 μg/ml BSA, and then incubated with 4 μM Btn-Pγ by rotating the microcentrifuge tube for 10 min at room temperature. A high concentration (1 μg/μl) of BSA or soybean trypsin inhibitor was added at this step to block possible nonspecific protein-bead interactions. After this incubation, Btn-Pγ was found completely bound to the streptavidin beads (data not shown). To test if the Pγ peptides disrupt the Pγ-α_tGTPγS or Pγ-P$\alpha\beta$ interaction, Pγ(62–87) or Pγ(1–61) in excess over Btn-Pγ was first incubated with α_tGTPγS or P$\alpha\beta$ in the pull-down buffer for 1 h on ice and then added to the Btn-Pγ-streptavidin beads. After rotating the reactions at 4 °C for 1–2 h, the beads were washed twice with 400 μl of ice-cold pull-down buffer. Proteins were then eluted from the beads with SDS/DTT-containing sample buffer, run on a low cross-link 15% acrylamide gel (33), and visualized by staining with Coomassie Blue R-250, or SilverSNAP Stain Kit II (Pierce) when lower amounts of proteins were used.

To study the interactions of the Pγ central region with P$\alpha\beta$ and α_t, the Pγ construct HisPγ(1–61) was used. For each reaction, 0.5 μl of His-Select High-Flow nickel beads (Sigma) were first washed with 500 μl of H_2O and then with 300 μl of pull-down buffer. HisPγ(1–61) of 5 μM was immobilized to the beads by incubation in the pull-down buffer (supplemented with 1 μg/μl trypsin inhibitor at this step) at room temperature for 10 min on rotating. Twenty mM imidazole was included in the pull-down buffer throughout the experimental procedures to prevent possible nonspecific binding of proteins to nickel beads. After the beads were washed with 2 × 500 μl of pull-down buffer to remove unbound HisPγ(1–61), P$\alpha\beta$ or/and α_tGTPγS were added and incubated with the beads for 1–2 h at 4 °C. The beads were then washed twice with 200 μl of pull-down buffer. The proteins on the beads were eluted with the sample buffer and resolved by SDS-PAGE using a low cross-link 15% gel (33), which was then silver-stained using SilverSNAP Stain Kit II (Pierce).

Immunoprecipitation Assay of the α_tGTPγS-PDE6 Interaction—Co-immunoprecipitation of α_tGTPγS with holo-PDE6 was carried out using nProtein A Sepharose Fast-Flow beads (Amersham Biosciences) and the antibody against bovine rod Pα (Affinity Bioreagents). For each reaction, 0.5 μl of Protein A beads were first equilibrated with the HEPES buffer (10 mM HEPES, pH 7.5, 120 mM NaCl, 5 mM $MgCl_2$) and then incubated with 0.5 μg of the anti-Pα antibody by rotating for 1 h at 4 °C. One μg/μl soybean trypsin inhibitor was included to block possible nonspecific protein binding sites on Protein A beads. The beads were washed three times with 300 μl of HEPES buffer prior to the immunoprecipitation reaction. Meanwhile, 0.5 μg of holo-PDE6 was incubated for 1–2 h on ice with 0.5 μg of α_tGTPγS in the HEPES buffer containing 50 μg/ml trypsin inhibitor and 1 mM DTT. The reaction was then added to the washed Protein A beads with anti-Pα bound and incubated for 1 h by rotating at 4 °C. Pγ peptide Pγ(1–61) or Pγ(62–87) in a 200-fold molar excess over holo-PDE6 was added as a competitor to disrupt Pγ interactions. After washing the beads three times with 300 μl of HEPES buffer (containing trypsin inhibitor and DTT), the immunoprecipitate was eluted with the sample buffer and subjected to SDS-PAGE and then detected by Western blotting using the anti-α_t antibody (K-20, Santa Cruz Biotechnology, Inc. (Santa Cruz, CA)).

Co-immunoprecipitation of P$\alpha\beta$ with α_tGTPγS was performed similarly but in a reverse manner. Briefly, 1.5 μg of anti-α_t was immobilized onto 0.75 μl of Protein-A beads. In separate tubes, 0.95 μg of P$\alpha\beta$ was incubated with 0.1 μg of Pγ on ice for 0.5 h with or without a competitor (Pγ(1–61) or Pγ(62–87) in a 200-fold molar excess over P$\alpha\beta$), and 0.2 μg of α_tGTPγS was then added. Following incubation on ice for 1 h, the reaction was mixed with washed anti-α_t/Protein A beads and rotated for 1 h at 4 °C. The P$\alpha\beta$ immunoprecipitate was

then eluted off of the washed beads and detected by Western blotting using the anti-Pα antibody.

Western Blot—Western blotting was performed as described previously (16). Low cross-link 15% acrylamide gels (33) were used for SDS-PAGE. Proteins were electrotransferred from the gel to the polyvinylidene difluoride membrane for 2 h at 45 V. Antibody dilutions were as follows: anti-Pα (Affinity Bioreagents), 1 μg/ml; anti-α_t (Affinity Bioreagents), 0.5 μg/ml; horseradish peroxidase-conjugated goat anti-rabbit secondary antibody (Sigma), 100,000–300,000-fold. The Millipore Immobilon Western horseradish peroxidase substrate was used for chemiluminescence detection of the horseradish peroxidase-labeled bands.

RESULTS

Profiling of the α_tGTPγS Interaction with the Full-length Pγ—A full spectrum profiling of Pγ-α_t interaction has not been reported. Previous peptide mapping studies showed that C-terminal Pγ peptides had slightly lower affinity for α_tGTPγS than peptides from the central region (17, 18). The affinity of these peptides with activated α_t (~1 μM), however, is nearly 100-fold lower than the full-length Pγ (10–12 nM (18, 34)). This conspicuous affinity difference indicates that the full-length Pγ molecule is required to assume an optimal conformation for binding with α_t. Obviously, peptide mapping is not an optimal approach to measure relative Pγ domain contributions in the full-length Pγ-α_tGTPγS interaction. Our label transfer experiments, in which the full-length Pγ could be used, however, offered a better means to address this issue.

Eleven photoprobes were prepared, with [^{125}I]ACTP site-specifically attached through mixed disulfide to the single cysteines placed at various positions throughout the Pγ molecule. Functional properties of these ACTP-Pγ probes have been carefully characterized when previously used to map the Pγ-P$\alpha\beta$ interaction interface, and no major change due to the ACTP modification was observed for the PDE6 inhibition potency of Pγ (28). A possible impact of ACTP on the Pγ function of α_t GTPase stimulation was further assessed in this study, which showed that the functional activities of these Pγ photoprobes were similar to that of the unmodified native Pγ (supplemental Fig. S1*B*).

We therefore used these probes in the photocross-linking/label transfer experiments to profile the Pγ-α_tGTPγS interaction. Upon UV illumination, the azide group of ACTP is photoactivated into a nitrene (35), which then inserts into the nearby Pγ-interacting site(s) on α_t, forming a covalent bond with the α_t backbone. After DTT reversal of the S–S link between ACTP and the cysteine on Pγ, the ^{125}I radiolabel is transferred from Pγ to α_t (see the diagram in supplemental Fig. S1*A*), which can be detected by autoradiography (Fig. 1*A*). Thus, the label transfer efficiency reflects the interaction intensity between α_t and a given Pγ position where [^{125}I]ACTP is attached.

The [^{125}I]ACTP-Pγ photoprobes, which were previously proven to transfer radiolabel to P$\alpha\beta$ specifically (28), were shown here to also specifically transfer radiolabel to α_tGTPγS. Specificity of the observed label transfer to α_t was manifested not only by the absence of radiolabel on BSA (Fig. 1*A*), which was included as an internal control, but also by the Pγ position dependence of label transfer (Fig. 1*B*).

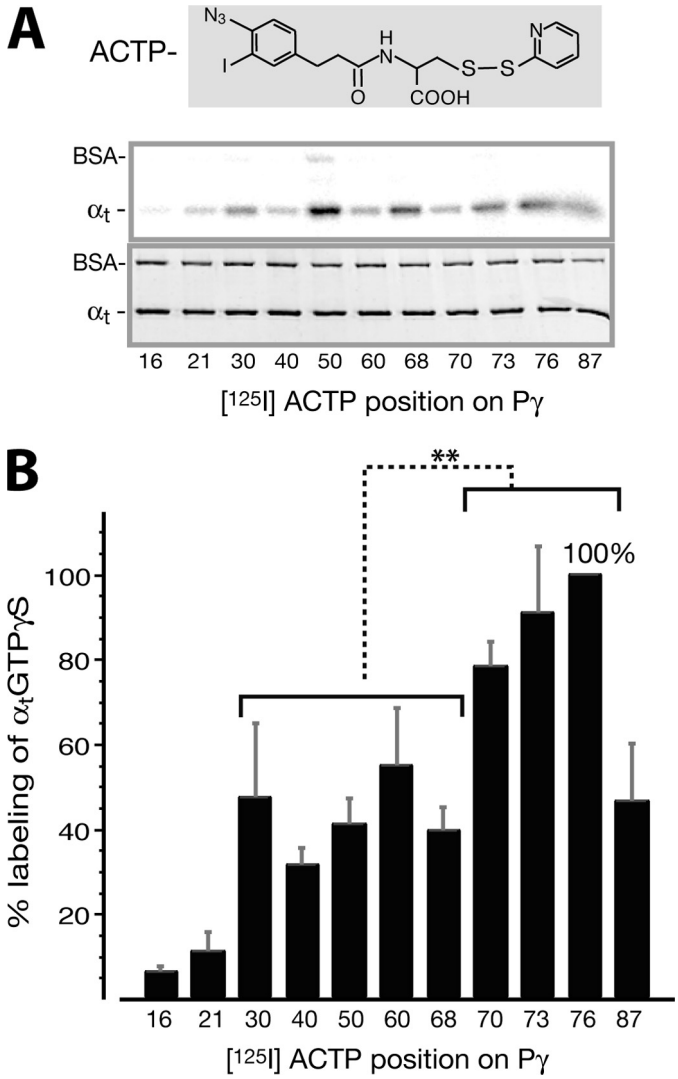

FIGURE 1. **Profiling of [^{125}I]ACTP label transfer to α_tGTPγS from various positions throughout the Pγ molecule.** *A*, radiolabel transfer from [^{125}I]ACTP-Pγ to α_tGTPγS was detected by autoradiography (*top panel*). Shown in the *bottom panel* is the Coomassie-stained gel, *below* which the corresponding [^{125}I]ACTP derivatization positions on Pγ are listed. Photocross-linking reactions were performed with 1 μM α_tGTPγS and 0.8 μM [^{125}I]ACTP-Pγ (see "Experimental Procedures"). BSA was included in the reactions as an internal control. *B*, profile of quantified label transfer to α_tGTPγS. Each data value is expressed as a percentage relative to the maximum labeling (position 76, ±15.7%) and presented as an average ±S.D. (*error bars*) of four separate experiments. The amount of label transfer to α_tGTPγS from each Pγ position was normalized for the α_t protein amount and the specific activity of the corresponding [^{125}I]ACTP-Pγ probe (supplemental Table S1 or Ref 28). Statistical analyses were performed by *t* test (Microsoft Excel). *, p = 0.01–0.05 (significant); **, p = 0.001–0.01 (very significant); ***, $p < 0.001$ (extremely significant); *ns*, $p > 0.05$ (not significant). As shown in the figure, there is a very significant difference between label transfer from the Pγ Phe^{30}–Cys^{68} region and that from the Trp^{70}–Leu^{76} region. Position 87 is not included in the latter group for statistical analysis because label transfer from the hydrophilic ACTP probe substituting the hydrophobic Ile^{87} residue could not accurately reflect the interaction between this position and α_tGTPγS (see the discussion of Figs. 1 and 2 under "Results"). The difference between each position and position 76 is also analyzed: positions 16 and 21 (***); 40, 50, and 68 (**); 30, 60, and 87 (*); 70 and 73 (not significant).

The label transfer yield from each Pγ position was quantified by normalizing the intensity of radiolabel on α_t with the specific radioactivity of the corresponding [^{125}I]ACTP-Pγ photoprobe

(supplemental Table S1) (28). Interestingly, the resultant profile of label transfer to α_t showed a pattern in which α_tGTPγS was highly labeled by [^{125}I]ACTP from the Pγ C-terminal positions around Trp^{70} (positions 70, 73, and 76) (Fig. 1*B*). This region is known to have intimate contacts with α_t (20). [^{125}I]ACTP from the Pγ central positions Phe^{30}-Leu^{60} (and the C-terminal position Ile^{87}), however, only moderately labeled α_tGTPγS. A low level of label transfer from the Pγ N-terminal positions 16 and 21 most likely represents a background level. Consistently, experiments performed under the same conditions but using α_tGDP-AlF_4^-, which shares a high similarity with α_tGTPγS in their three-dimensional structures and functional properties (20, 36), showed a similar profiling pattern of label transfer (data not shown).

To further confirm the observed Pγ-α_tGTPγS interaction pattern (Fig. 1*B*), label transfer profiling was also carried out using Pγ photoprobes containing mBP, a photoreactive group different from ACTP (Fig. 2*A*). Under UV light (350–365 nm), the ketone in benzophenone is activated into a diradical by disproportionation and reacts with neighboring C–H bonds (35) in α_t to form a C–C link. Because the maleimide group forms a C–S bond with the cysteine on Pγ, which cannot be cleaved by DTT, the cross-linked Pγ-α_t complex stays covalently linked and migrates as a band higher than the α_t band on the gel after SDS/DTT treatment (Fig. 2*A*). The mBP-Pγ photoprobes, which have been previously characterized, showed no significant functional changes in PDE6 inhibition due to mBP modifications on Pγ (16). Moreover, in a previous study from our laboratory (29), another benzophenone probe, benzoyl-L-phenylalanine, which is very similar to mBP, caused only minor changes in the Pγ stimulation of α_t GTPase when incorporated into a Pγ C-terminal position at 66, 73, 76 or 86.

In a good agreement with the above results of [^{125}I]ACTP label transfer, the cross-linking experiments using mBP-Pγ resulted in a similar profiling pattern (Fig. 2*B*). Thus, the fact that profiling with two different photophores (ACTP and mBP) led to similar patterns eliminates concerns regarding possible chemical selectivities of the photoprobes.

Compared with [^{125}I]ACTP-Pγ, the mBP-Pγ probes showed a more profound preference for the Pγ C-terminal positions in cross-linking with α_tGTPγS. This difference very likely stemmed from the fact that mBP is more hydrophobic (than ACTP) and thus more similar to the C-terminal hydrophobic residues that were replaced by the photoprobe. An interesting example is Ile^{87}, the prominent hydrophobicity of which is known to play an important role in the function of Pγ (12, 13). Accordingly, the hydrophobic mBP at position 87 yielded the highest Pγ-α_tGTPγS cross-link efficiency (Fig. 2*B*), whereas [^{125}I]ACTP, a relatively hydrophilic probe due to the presence of a carboxyl group (Fig. 1*A*), resulted in less cross-link efficiency at position 87 (Fig. 1*B*). In this regard, the mBP cross-linking profile (Fig. 2*B*) may better represent Pγ domain contributions to the Pγ-α_tGTPγS interaction.

Notably, both [^{125}I]ACTP and mBP yielded a substantial cross-link at Pγ position 70 (Figs. 1*B* and 2*B*), which is critical for the Pγ-α_t interaction (20). This observation agrees with our previous study in which benzoyl-L-phenylalanine replacement

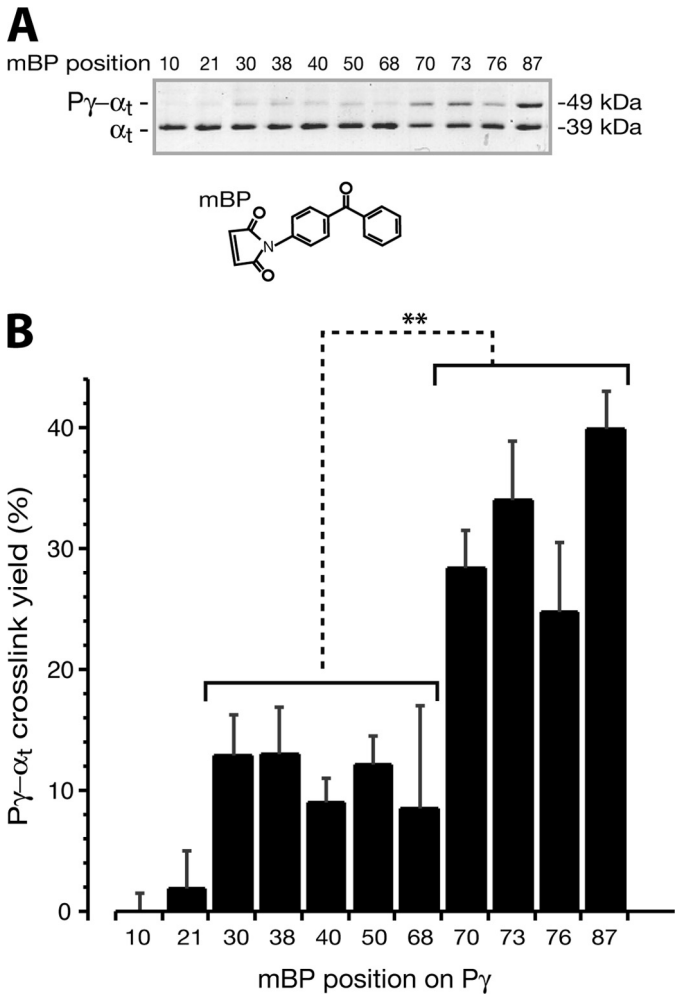

FIGURE 2. **Profiling of the Pγ-α_tGTPγS interaction using mBP photoprobes.** *A*, photocross-linked mBP-Pγ-α_tGTPγS is shown as a higher band above the α_t band on the Coomassie-stained SDS gel. The photocross-linking reactions were performed as described under "Experimental Procedures." Each reaction included 1.6 μg of α_tGTPγS and an equal molar amount of mBP-Pγ in the HEPES buffer (10 mM HEPES, pH 7.5, 120 mM NaCl, 5 mM $MgCl_2$). DTT was added at a concentration of 2 mM to prevent possible nonspecific cross-link. *B*, the photocross-link efficiency of mBP-Pγ and α_tGTPγS at each Pγ position was quantified as a percentage ratio of the protein amount in the cross-link band *versus* the sum in both the α_t band and the cross-link band. Each *bar* represents an average ± S.D. (*error bars*) of six separate experiments. The mBP derivatization positions on Pγ are listed at the *bottom*. The difference in cross-link efficiency of α_tGTPγS with two groups of Pγ positions, Phe^{30}–Cys^{68} and Trp^{70}–Ile^{87}, is very significant. *t* test of each position against position 87 is shown: positions 10, 21, 30, 38, 40, 50, and 68 (***); positions 70 and 76 (**); and position 73 (not significant (*ns*)).

of Trp^{70} also yielded a relatively high cross-link efficiency (29). The simplest explanation is that, due to a similarity to tryptophan, the photoprobe placed at position 70 could remain in close proximity to the Trp^{70}-interacting residues of α_tGTPγS. This proposition is also supported by the native gel assay in which the ACTP-Pγ·α_t complexes still formed substantially, although the ACTP derivatization at position 70, 76, or 87 affected the Pγ·α_t interaction to some extent (supplemental Fig. S1*C*). It is thus reasonable to conclude that the α_tGTPγS interaction with Trp^{70} would be actually stronger than observed here with a photoprobe substitution at this position. Nevertheless, our profiling experiments using full-length purified proteins revealed a clear pattern of the Pγ-α_tGTPγS inter-

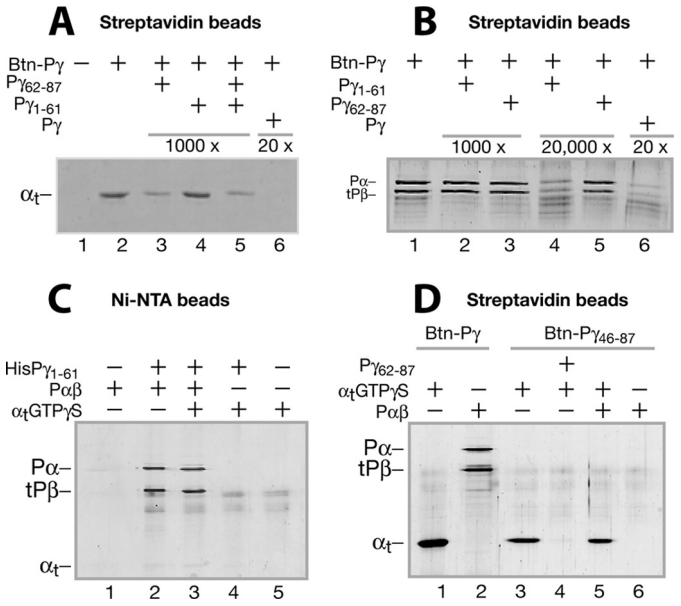

FIGURE 3. **Differential Pγ domain interactions with α_tGTPγS and P$\alpha\beta$ evidenced by pull-down experiments.** Pull-down experiments were performed with Btn-Pγ or Btn-Pγ(46–87) immobilized on strepavidin beads or HisPγ(1–61) immobilized on Ni^{2+}-nitrilotriacetic acid beads. Conditions are described under "Experimental Procedures" unless otherwise stated. Trypsin inhibitor instead of BSA was included to block nonspecific protein-bead interactions because BSA (66 kDa) migrates too close to tPβ (~70 kDa) on the gel. The gels in *A–D* each represent at least three similar experiments. *A*, pull-down of α_tGTPγS by Btn-Pγ. The control without Btn-Pγ is shown in *lane 1*. The Pγ peptide Pγ(62–87) (*lane 3*), Pγ(1–61) (*lane 4*), or both (*lane 5*) in a 1000-fold molar excess over Btn-Pγ or the full-length Pγ in a 20-fold excess (*lane 6*) was added to compete with the Btn-Pγ-α_tGTPγS interaction. *B*, pull-down of P$\alpha\beta$ by Btn-Pγ. Pγ(1–61) (*lanes 2* and *4*) or Pγ(62–87) (*lanes 3* and *5*), in a 1000- or 20,000-fold molar excess over Btn-Pγ, was present, competing with the Btn-Pγ-P$\alpha\beta$ interaction. *C*, pull-down of P$\alpha\beta$ or α_tGTPγS using the HisPγ(1–61) peptide immobilized to nickel beads. *Lanes 1* and *5*, controls without HisPγ(1–61) for pulling down P$\alpha\beta$ (*lane 2*) and α_tGTPγS (*lane 4*), respectively. Both P$\alpha\beta$ and α_tGTPγS were added in the reaction of *lane 3*. *D*, pull-down of α_tGTPγS (*lanes 3* and *4*) or P$\alpha\beta$ (*lane 6*) by Btn-Pγ(46–87). Pγ(62–87) in a 200-fold molar excess over Btn-Pγ(46–87) was used to compete with the Btn-Pγ(46–87)-α_tGTPγS interaction. Pull-down of α_tGTPγS (*lane 1*) or P$\alpha\beta$ (*lane 2*) by the full-length Btn-Pγ was also performed to compare with the Btn-Pγ(46–87) pull-down conditions.

action; the C-terminal domain of Pγ contributed the major strength for the interaction with α_tGTPγS compared with the remainder of the Pγ molecule (Figs. 1*B* and 2*B*).

The C-terminal Domain of Pγ Provides Major Binding Strength for the Pγ Interaction with α_tGTPγS, as Does the Central Domain for the Interaction with P$\alpha\beta$—In order to further assess the role of the Pγ C-terminal domain in the interaction with α_tGTPγS, a different approach (pull-down) was applied, using Btn-Pγ bound to streptavidin beads. As shown in Fig. 3*A*, α_tGTPγS was specifically pulled down by Btn-Pγ (*lane 2*), because no α_t was detected in the control with no Btn-Pγ (*lane 1*). Interestingly, the Pγ C-terminal peptide Pγ(62–87) effectively abolished α_tGTPγS pull-down (*lane 3*), but the N-terminal peptide Pγ(1–61) of the same concentration did not (*lane 4*). This result demonstrates a dominant role of the Pγ C-terminal domain in the Pγ-α_tGTPγS interaction. This conclusion is also supported by the observation that the C-terminal half of Pγ (Btn-Pγ(46–87)) efficiently pulled down α_tGTPγS (Fig. 3*D*, *lane 3*), but the N-terminal HisPγ(1–61) peptide did not (Fig. 3*C*, *lane 4*). Importantly, the observation that the Pγ C-terminal domain provided the major Pγ-α_tGTPγS interaction strength (Figs. 1–3) is in accord with the crystal structure of the partial GAP complex (20), in which the Pγ C-terminal domain is engaged in a hydrophobic interlock between the $\alpha_{t/i1}$ switch II and α_3 helix.

It is noteworthy that the full-length Pγ in a 20-fold excess completely abolished the α_tGTPγS pull-down (Fig. 3*A*, *lane 6*), and the full-length Pγ pulled down α_tGTPγS much more efficiently than the C-terminal half-peptide (compare *lane 1* with *lane 3* in Fig. 3*D*). This is consistent with the previous assessment that although either the central or the C-terminal peptides could interact with α_tGTPγS separately, the full-length Pγ interacted with α_t with a much higher affinity (17, 18). Here we further assert that in the full-length Pγ-α_t interaction, although the C-terminal domain contributes more than the central domain, both domains are required to forge a strong Pγ-α_tGTPγS interaction.

Interestingly, in contrast to the major role of the Pγ C-terminal domain in the Pγ-α_t interaction, it is Pγ(1–61) (Fig. 3*C*, *lane 2*) rather than the C-terminal half (Fig. 3*D*, *lane 6*) that efficiently pulled down P$\alpha\beta$. The fact that Pγ(1–61) (*lane 4* in *B*) but not Pγ(62–87) (*lane 5* in *B*) abrogated the Pγ-P$\alpha\beta$ interaction also indicates a dominant role of the Pγ N-terminal side for interacting with P$\alpha\beta$. This conclusion is consistent with the previous observations that the Pγ central domain binds P$\alpha\beta$ much more strongly than the C-terminal domain (14). It is noteworthy that Pγ(1–61) that was 20,000-fold (*lane 4* in *B*) but not 1000-fold (*lane 2* in *B*) in molar excess could disrupt the Pγ-P$\alpha\beta$ interaction. This result reflects an exceptionally tight full-length Pγ-P$\alpha\beta$ interaction, the optimum K_d of which is in the subpicomolar range (1, 14). Therefore, the stark contrast of the binding of P$\alpha\beta$ and α_tGTPγS to the same Pγ domain raised an important question as to whether Pγ interacts with α_tGTPγS and P$\alpha\beta$ differentially.

Pγ Interacts with α_tGTPγS and P$\alpha\beta$ in a Complementary Manner—Label transfer profiling with the full-length, photoprobe-derivatized Pγ constructs allowed us to compare the pattern of Pγ-α_tGTPγS interaction (Figs. 1*B* and 2*B*) with the previously observed Pγ-P$\alpha\beta$ interaction profile (28). A "complementary" feature of the two separately determined profiles was thus revealed, in which the Pγ central region provides most of the strength for binding with P$\alpha\beta$, whereas the C-terminal region accounts for the major interaction with α_tGTPγS. These data prompted us to investigate the competition between α_tGTPγS and P$\alpha\beta$ for interacting with Pγ, by comparing the [^{125}I]ACTP label transfer to α_tGTPγS and to P$\alpha\beta$ from various Pγ positions in a systematic manner. For this purpose, label transfer to α_tGTPγS and P$\alpha\beta$ from a certain Pγ position in a photocross-linking reaction with these two partners present could be directly compared in the same *lane* on the SDS gel (Fig. 4*A*). These experiments were intended to mimic the signaling state when α_tGTP interacts with and displaces Pγ from PDE6 to activate the enzyme. Pγ was utilized substoichiometrically in comparison with α_tGTPγS and P$\alpha\beta$ (0.7 Pγ, 1 α_t, 1 subunit of P$\alpha\beta$) so that α_tGTPγS and P$\alpha\beta$ could effectively "compete" in their interactions with Pγ and therefore provide a greater opportunity for revealing a preferential labeling on α_tGTPγS or P$\alpha\beta$ from a given Pγ position. As shown in the autoradiogram (Fig. 4*A*) and the data that are summarized as the labeling ratios

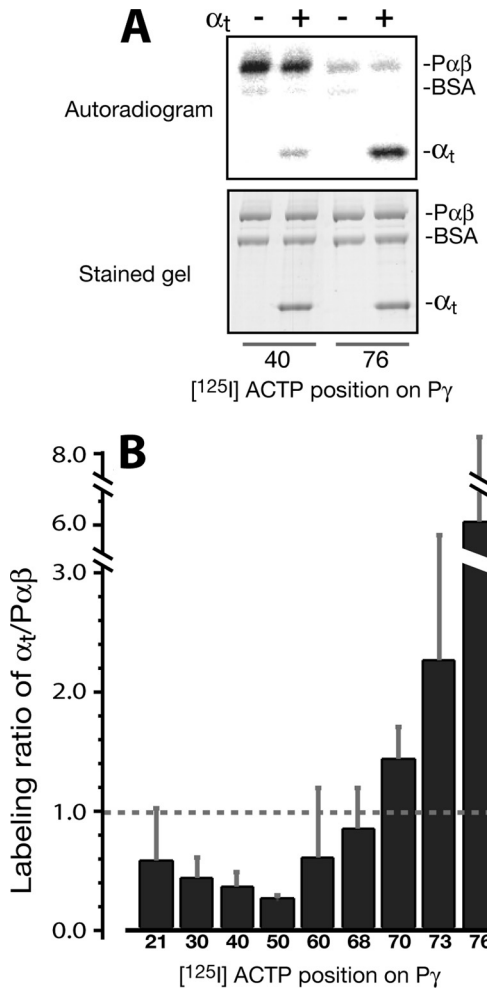

FIGURE 4. **Distinct Pγ domain preference of label transfer to α_tGTPγS and Pαβ competing for interaction with Pγ.** *A*, label transfer from the [^{125}I]ACTP-Pγ photoprobes to α_tGTPγS in competition with Pαβ. [^{125}I]ACTP-Pγ photoprobes of the same batch as in Fig. 1 were used. Photocross-linking reactions were conducted with the [^{125}I]ACTP-Pγ photoprobes in the presence of both α_tGTPγS (4 μM) and Pαβ (without a nick) at a molar ratio of 0.7 Pγ, 1.0 α_t, 1.0 Pαβ subunit. The reactions were then subjected to SDS-PAGE (*bottom*) and autoradiography (*top*). BSA was used as an internal control to demonstrate the specificity of label transfer. *B*, labeling ratio of α_tGTPγS *versus* Pαβ. Each *bar* value represents a mean ± S.D. (*error bars*) (of 3–5 experiments). The amount of label transfer to α_tGTPγS or Pαβ from each Pγ position was normalized for the α_t (or Pαβ) protein amount and the specific activity of the corresponding [^{125}I]ACTP-Pγ probe (supplemental Table S1 and Ref. 28). A *t* test was performed for each position against the value 1.0 (*dashed line*): positions 40, 50, and 76 (***); positions 30 and 87 (**); positions 70 and 73 (*); and positions 21, 60, and 68 (not significant (*ns*)). A bar value less than 1 indicates a labeling preference for Pαβ; accordingly, a value greater than 1 indicates a preference for α_t.

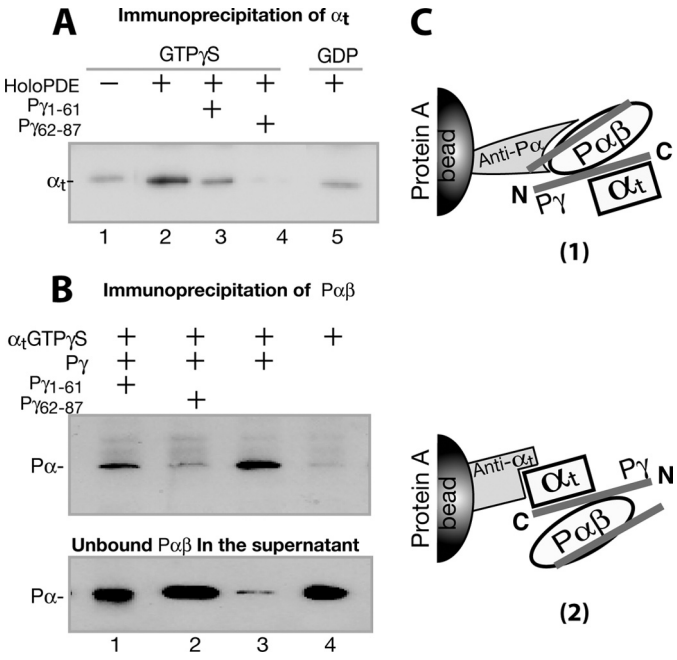

FIGURE 5. **Pγ-dependent α_t·PDE6 interaction detected through immunoprecipitation.** The immunoprecipitation experiments were conducted using purified proteins, antibodies, and Protein A beads, as described under "Experimental Procedures." The blots shown in the figure each represent at least three similar experiments. *A*, α_tGTPγS was immunoprecipitated by the holo-PDE6·anti-Pα·Protein A beads (*lane 2*). *Lane 1*, the control with no holo-PDE6. Pγ peptide Pγ(1–61) (*lane 3*) or Pγ(62–87) (*lane 4*) in a 200-fold molar excess was added to compete with the Pγ interactions. In *lane 5*, α_tGDP instead of α_tGTPγS was used. *B*, Pαβ was immunoprecipitated by the α_tGTPγS·anti-α_t·Protein A beads (*lane 3*). *Lane 4* is the control in the absence of Pγ. In *lanes 1* and *2*, Pγ(1–61) and Pγ(62–87) of 200-fold molar excess were added, respectively, to compete with the Pγ interactions. Immunoblotting of supernatants containing unbound Pαβ is shown in the *bottom panel*. *C*, diagrams depicting the experimental strategies in *A* and *B*. For simplicity, the second α_t molecule that could also bind to Pγ·Pαβ (46) is not shown.

for the two targets (Fig. 4*B*), a distinct preference of photolabel transfer for α_tGTPγS over Pαβ occurred from the Pγ C-terminal positions, in particular from position 76. Accordingly, the recent crystal structure (5) showed that whereas the Pγ C terminus bound to the chimeric PDE5/6 catalytic domain, Leu^{76} pointed away, positioning itself in a direction ready for interaction with α_t. In clear contrast to the C-terminal positions, however, more labeling from the Pγ central positions (Val^{21}–Leu^{60}) was observed on Pαβ than on α_tGTPγS (Fig. 4*B*). These experiments of label transfer competition further confirm the complementary nature of the Pγ interactions with α_tGTPγS and Pαβ, which was first exhibited by the different interaction profiles.

Complementary Pγ Interactions with α_t and Pαβ Constitute the α_t·PDE6 Complex—Given the above evidence that Pγ differentially interacted with its two targets, with the C-terminal domain favoring α_tGTPγS and the central region preferring Pαβ, we sought to test whether the complementary interactions play an important role in the intermediate transducin·PDE6 complex, using co-immunoprecipitation approaches (Fig. 5, *A* and *B*). If the α_tGTPγS·PDE6 complex is indeed primarily held together by the Pγ C-terminal interaction with α_tGTPγS and the central region interaction with Pαβ (diagramed in Fig. 5*C*), disrupting either of these interactions using a Pγ peptide should dissociate the α_t·PDE6 complex.

We first observed that α_tGTPγS was co-immunoprecipitated specifically with the holo-PDE6 that was immobilized to Protein A beads via the anti-Pα antibody (Fig. 5*A*, *lane 2*), as compared with the control with no holo-PDE6 added (*lane 1*). The immunoprecipitation of α_t proved to be GTP-dependent because only a background level of α_tGDP was co-immunoprecipitated with holo-PDE6 (*lane 5*). Moreover, the α_t precipitation diminished in the presence of either Pγ(1–61) (*lane 3*) or Pγ(62–87) (*lane 4*), indicative of complementary Pγ interactions with α_t and Pαβ.

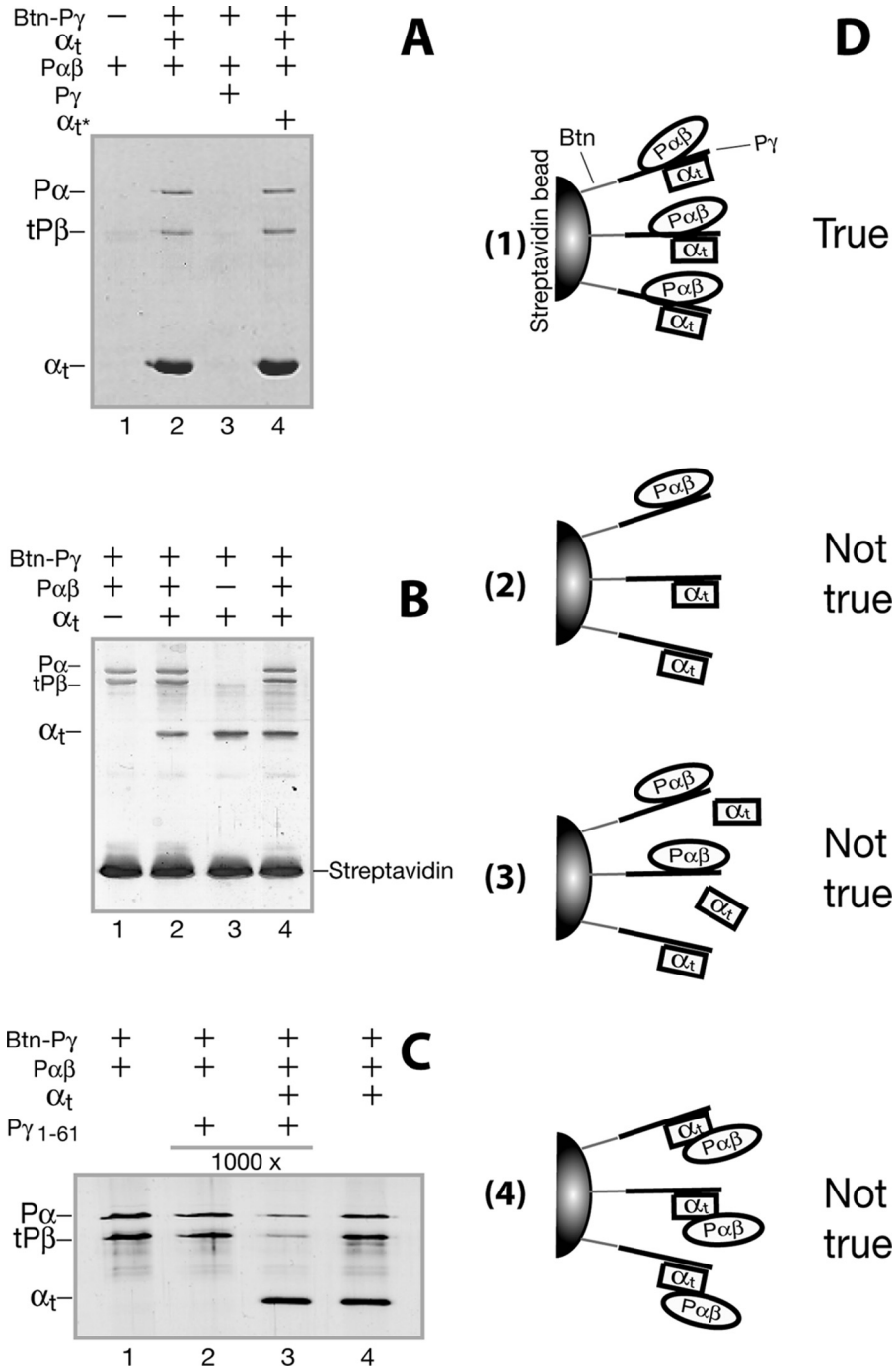

FIGURE 6. **Simultaneous Pγ binding with α_tGTPγS and P$\alpha\beta$ evidenced by pull-down experiments.** Pull-down was performed as described under "Experimental Procedures." Trypsin inhibitor was used to block nonspecific protein-bead interactions. 4 μM Btn-Pγ was used in *A*, and the gel was Coomassie-stained; 0.5 μM Btn-Pγ was used in *B* and *C*, and the gels were silver-stained. Each gel shown in the figure is a representative of at least three similar experiments. *A*, α_tGTPγS in a 5-fold molar excess *versus* Btn-Pγ (4 μM) was added to the Btn-Pγ streptavidin beads to saturate the α_t-binding sites on Btn-Pγ by incubation for 1 h at 4 °C. After washing the beads, P$\alpha\beta$ (0.2 μM dimer) was added and incubated for another 1 h. In the reaction of *lane 3*, Pγ in 5-fold molar excess was added to compete with the Btn-Pγ-P$\alpha\beta$ interaction. In *lane 4*, α_tGTPγS in a 5-fold molar excess was added *again* (marked as α_t*) after washing the α_t-saturated Btn-Pγ beads to resaturate the Pγ molecules that could have become free due to extensive washing. *B*, in order to determine whether α_t could replace P$\alpha\beta$ that is prebound with Btn-Pγ, the P$\alpha\beta$-binding sites of Btn-Pγ were first saturated by incubation with 1 μM P$\alpha\beta$, the beads were washed, and 1 μM α_tGTPγS (*lane 2*) or equal volume of pull-down buffer (*lane 1*) was then added. Similarly, to address whether P$\alpha\beta$ could replace α_t that is bound on the Btn-Pγ beads, the α_t-binding sites were first saturated with 2 μM α_tGTPγS, 1 μM P$\alpha\beta$ (*lane 4*), or an equal volume of pull-down buffer (*lane 3*) was then added after washing the beads. *C*, the P$\alpha\beta$-binding sites of Btn-Pγ were first saturated by incubation with 1 μM P$\alpha\beta$, and the effect of Pγ(1–61) on P$\alpha\beta$ pull-down was then compared in the absence (*lane 2*) or presence (*lane 3*) of 2 μM α_tGTPγS. *D*, schematic diagrams of alternative explanations for the co-pull-down of α_tGTPγS and P$\alpha\beta$ by Btn-Pγ. For ease in distinguishing the proteins, α_tGTPγS, P$\alpha\beta$, and Pγ are shown as *squares*, *ovals*, and *lines*, respectively.

To further explore the Pγ-dependent nature of the α_t·PDE6 co-immunoprecipitation, experiments were performed in a reverse manner, detecting co-immunoprecipitation of P$\alpha\beta$ with α_tGTPγS, which was immobilized on Protein A beads through the anti-α_t antibody (Fig. 5*B*). Similar to the results shown in Fig. 5*A*, P$\alpha\beta$ was co-immunoprecipitated with α_tGTPγS in the presence of Pγ (*lane 3*). Obviously, P$\alpha\beta$ was precipitated by the Pγ·α_tGTPγS complex, because no P$\alpha\beta$ precipitation was observed when Pγ was absent (*lane 4*). P$\alpha\beta$ precipitation was diminished in the presence of Pγ(1–61) (*lane 1*) or Pγ(62–87) (*lane 2*). A significant portion of P$\alpha\beta$ was still precipitated with excess Pγ(1–61) present (*lane 1*), reflecting tight binding of the Pγ N-terminal half with P$\alpha\beta$ (see Fig. 3, *B* and *C*). These data further confirm the Pγ-mediated complementary interactions.

With the data in Fig. 5 showing Pγ-dependent co-immunoprecipitation of α_tGTPγS with PDE6 as well as co-immunoprecipitation of PDE6 with α_tGTPγS, we obtained additional evidence (Fig. 6, *A–C*) supporting the conclusion that complementary and simultaneous binding of Pγ to its two partners constituted the α_t·PDE6 complex.

The experiments were designed based on the following idea. If P$\alpha\beta$ binds Pγ simultaneously along with α_tGTPγS (diagramed in Fig. 6*D*, *1*), P$\alpha\beta$ should be pulled down by the Btn-Pγ molecules on streptavidin beads that are saturated by excess α_tGTPγS, and *vice versa*. As shown in Fig. 6*A*, P$\alpha\beta$ was readily pulled down by Btn-Pγ, which was bound to the beads and preincubated with α_tGTPγS at a 5-fold molar excess (*lanes 2* and *4*), supporting the notion that co-binding of α_tGTPγS and P$\alpha\beta$ to Btn-Pγ occurred as depicted in Fig. 6*D*, *1*. We cautioned that the observed co-pull-down of P$\alpha\beta$ and α_t might be subject to such alternate explanations as depicted in Fig. 6*D*, *2–4*. However, these concerns can be ruled out by detailed analysis of our data. First, P$\alpha\beta$ was

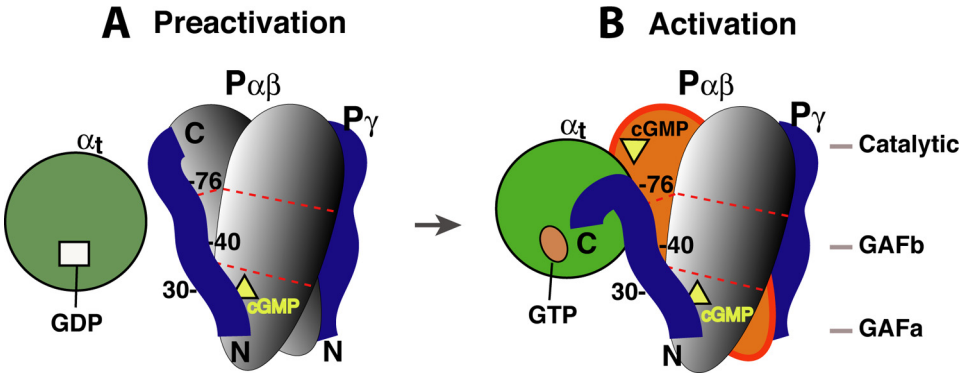

FIGURE 7. **Schematic diagram of the complementary Pγ interactions with its two targets during PDE6 activation.** The molecules involved in PDE6 activation are represented by different *shapes*. *Egg*, Pα and Pβ; *circle*, α_t; *ribbon*, Pγ; *square*, GDP; *oval*, GTP; *triangle*, cGMP. For simplicity, the three domains of Pα and Pβ are shown as segments separated by the *dotted red lines*. Our previous studies revealed that the Pγ Phe^{30} region preferred binding to Pα, whereas the Ser^{40} region favored binding to Pβ, suggesting simultaneous Pγ interactions with Pα and Pβ (16, 28). Because PDE6 can only be efficiently activated 50% by transducin (26, 46), it is highly likely that only one Pγ is displaced by α_tGTP during PDE6 activation in the mammalian retina, whereas the other Pγ (on the opposite side) stays tightly bound to Pαβ (1). A movement of the Pγ(78–87) segment from Pαβ to α_tGTP was suggested by Barren *et al.* (5), based on the crystal structure of the Pγ(70–87)·PDE5/6 catalytic domain complex.

not pulled down by a population of Btn-Pγ that could have become free due to extensive washing of the α_t-saturated beads (see Fig. 6*D*, *2*), because the same amount of Pαβ was pulled down in the presence of excess α_t that was added *back* to the α_t-saturated beads (Fig. 6*A*, *lane 4*). Second, the addition of Pαβ to α_t-saturated beads did not reduce α_t pull-down (Fig. 6*B*, compare *lane 4* with *lane 3*), indicating that the Pαβ pull-down *did not* result from replacement of a portion of α_t by the Pαβ binding to Btn-Pγ (see *D3*). In this case, replaced α_t should have been washed off and would have led to a lowered intensity of the α_t band. This was also true for the α_t pull-down on Pαβ-saturated beads (compare *lane 2* with *lane 1* in *B*). Third, Pαβ was *not* pulled down by directly interacting with α_t (see *D4*), because α_t was readily pulled down by Btn-Pγ(46–87) but Pαβ was not pulled down together with α_t (Fig. 3*D*, *lane 5*). Similarly, α_t was not pulled down together with Pαβ, which was pelleted with His-Pγ(1–61) on nickel beads (Fig. 3*C*, *lane 3*).

Finally, Pγ(1–61) in a 1000-fold excess could not compete with the strong full-length Pγ-Pαβ interaction (Fig. 3*B*, *lane 2*, and Fig. 6*C*, *lane 2*) but could do so in the presence of α_tGTPγS (Fig. 6*C*, *lane 3*). The simplest explanation is that simultaneous binding of α_tGTPγ to Btn-Pγ along with Pαβ weakened the Pγ-Pαβ interaction by sequestering the Pγ C-terminal domain and thus kept Pαβ from a high affinity binding with the full-length Pγ. Taken together, these lines of evidence suggest that Pγ facilitated the formation of the α_tGTPγS·PDE6 complex by binding to both Pαβ and α_tGTPγS simultaneously.

DISCUSSION

PDE6 activation mediated by α_t is the central step in the visual transduction cascade. How Pγ interacts with its two targets (α_t and Pαβ) is the key to understanding the molecular mechanism of PDE6 activation, yet it has been difficult to capture a snapshot of this dynamic process through structural biology. We have obtained evidence here supporting the conclusion that complementary interactions (a strong Pγ C-terminal interaction with α_tGTP and a tight binding of the central region to Pαβ) occur in favor of PDE6 activation and at least partly account for the binding force in the intermediate α_t·PDE6 complex.

It is known that the Pγ central region and the C-terminal domain are the two primary binding sites not only for α_tGTPγS but also for Pαβ (8, 10, 16–18, 29, 37, 38), but it is not yet clear how the two Pγ domains differentiate their interactions with α_t and Pαβ (9) when both targets are involved during PDE6 activation.

The observation of complementary Pγ domain interactions with α_tGTPγS and Pαβ was based on comparison of the interaction profiles with the two targets, both obtained from systematic mapping of the entire interaction interfaces. A stronger α_tGTPγS interaction with the Pγ C-terminal domain than with the Pγ central region (Figs. 1*B* and 2*B*) was in interesting contrast to a stronger Pαβ interaction with the Pγ central region than with the Pγ C-terminal domain (28), as also indicated by the pull-down experiments (Fig. 3). More significantly, this complementary feature was also observed when both of the targets were present competing for Pγ interaction (Fig. 4).

The complementary Pγ interactions with its two targets may have important implications for the molecular mechanism of PDE6 activation. The significance is 2-fold. First, because the α_t-interacting C-terminal domain (Thr^{62}–Ile^{87}) includes the PDE6-inhibiting region, a strong Pγ C-terminal interaction with α_tGTP is essential to compete with the Pγ-Pαβ interaction in order to displace the Pγ C terminus from the Pαβ catalytic site (5, 8, 20). Accordingly, a weak interaction between the Pαβ catalytic domain and the Pγ C-terminal domain should therefore provide α_tGTP a stronger competitive edge over Pαβ, ensuring an efficient PDE6 activation. Moreover, tight binding of the Pγ C-terminal domain to α_tGTP helps keep Pγ from reinhibiting PDE6 before the visual signal is adequately amplified (20).

Second, a greater binding strength of Pαβ for the Pγ central region keeps it sequestered by Pαβ. Because it is the complex formed by α_tGTP and the full-length Pγ that can be readily recognized by RGS9-1·Gβ5 to maximally fulfill the GAP function (32), sequestration of the Pγ N-terminal half by Pαβ may prevent visual signaling from being terminated too early. An extremely high rod visual sensitivity is thus achieved not only because of an exceptionally high efficiency of the activated PDE6 but also for its extended lifetime (1).

Furthermore, the complementarity of the Pγ-α_t interaction and the Pγ-Pαβ interaction also reveals some insights with regard to the molecular topology of the α_t·PDE6 complex. α_tGTPγS was co-immunoprecipitated by holo-PDE6, and Pαβ was co-immunoprecipitated by α_tGTPγS, all in a Pγ-dependent fashion (Fig. 5). This indicates a molecular organization

such that the C-terminal domain of Pγ binds tightly with α_tGTPγS while the central region forms a strong interaction with Pαβ, thus "gluing" α_tGTPγS and Pαβ into the PDE6 activation complex, or "transducisome." This proposed organization is also supported by the data from co-pull-down of α_tGTPγS and Pαβ by Btn-Pγ (Fig. 6). Thus, the complementary Pγ interactions may explain a long held puzzle; although the Pαβ-binding regions and α_t-binding regions overlap on Pγ (1, 9), an intermediate transducin·PDE6 complex could still occur during visual transduction (22–24). Our data do not exclude the possibility that in the PDE6 activation complex, the Pγ central region may also be involved in binding with α_tGTP, albeit probably through weak interactions. A mutagenesis study showed that Lys^{41}, Lys^{44}, and Lys^{45} on the C-terminal side of the Pγ polycationic region were involved in the interaction with α_t but not with Pαβ (39), raising the possibility of simultaneous non-competitive α_tGTPγS and Pαβ binding to the Pγ central region.

Early studies using rod disc membranes suggested that direct α_t-Pαβ interaction accounted for an important binding force in the α_t·PDE6 complex (24, 27). In the current study, however, α_tGTPγS and Pαβ were not co-immunoprecipitated with each other in the absence of Pγ (Fig. 5). Moreover, when either α_tGTPγS or Pαβ was bound to Btn-Pγ(46–87) or HisPγ(1–61) on affinity beads, the other was not co-pulled down (Fig. 3). These results indicate a lack of direct α_t-Pαβ interaction in the α_t·PDE6 complex under our experimental conditions. Because no disc membranes were involved in our experiments, we suggest that the disc membranes used in the early studies may have played a role in organizing the proteins in such a way that α_t and Pαβ make direct contacts that further tighten the α_t·PDE6 complex. In support of this proposition, increasing evidence indicates that disc membranes enhance protein functions in phototransduction (40–42). Nevertheless, our data indicate that the complementary Pγ interactions with its two targets, at least in part, account for the binding force in the α_t·PDE6 complex.

Based on the data presented herein and evidence from previous studies, a possible scenario of protein-protein interactions during PDE6 activation is depicted in Fig. 7. GTP-bound α_t may initially engage PDE6 by making contacts with the Pγ residues Trp^{70} and Leu^{76}, which are not involved in intimate interactions with the Pαβ catalytic site (5, 8, 11), and may also interact via part of the polycationic region (19, 39) (Figs. 1*B* and 2*B*). These initial α_t contacts with Pγ may trigger a conformational change that results in a rigid body movement of the Pγ C terminus away from the Pαβ catalytic site with Leu^{76} serving as a "hinge." The Pγ C-terminal domain can now bind tightly with α_t, and PDE6 is deinhibited (5). At this stage, an intermediate complex containing α_tGTP·Pγ·Pαβ, or transducisome, probably exists due to the complementary binding of Pγ to α_tGTP and Pαβ (Figs. 4–6), with the Pγ C-terminal domain tightly bound to α_tGTP and the central region bound to the Pαβ GAF domain with high affinity. The Pγ central region could stay bound to the Pαβ GAF domain until the binding is weakened by lowered cGMP levels, through a mechanism of positive cooperativity of Pγ and non-catalytic cGMP in binding to the GAF domain (1, 14, 26, 43, 44).

Thus, the duration of the α_tGTP·Pγ·Pαβ transducisome is probably subject to regulation by the cGMP occupancy in the Pαβ GAF domain. However, the activity of the GAP complex may have a more significant effect on the lifetime of the transducisome, because GTP hydrolysis in α_t accelerated by RGS9-1 is the rate-limiting step of the rod photoresponse (45). Interesting questions hereby arise as to how Pγ dynamically and differentially interacts with RGS9-1/Gβ5, α_t, and Pαβ upon a transition from its role in the PDE6 activation complex to that in the GAP complex and how the cGMP binding in the GAF domain regulates this process. Because disruption of Pγ interactions with its partners in phototransduction causes impaired visual functions (9), systematic investigations of these interactions will advance our understanding of the molecular mechanisms of the related retinal diseases.

Acknowledgments—We thank K. A. Martemyanov and V. Y. Arshavsky for functional assays of the Pγ photoprobes and H. Muradov and N. O. Artemyev for the PDE6 preparations. We also thank M. Arbabian for help in radiosynthesis and transducin preparations and M. M. Vestling for assistance in mass spectrometry.

REFERENCES

1. Cote, R. H. (2006) *Photoreceptor Phosphodiesterase (PDE6): A G-protein-activated PDE Regulating Visual Excitation in Rod and Cone Photoreceptor Cells*, pp. 165–193, CRC Press, Inc., Boca Raton, FL
2. Oldham, W. M., and Hamm, H. E. (2008) *Nat. Rev. Mol. Cell Biol.* **9,** 60–71
3. Burns, M. E., and Arshavsky, V. Y. (2005) *Neuron* **48,** 387–401
4. Artemyev, N. O., Arshavsky, V. Y., and Cote, R. H. (1998) *Methods* **14,** 93–104
5. Barren, B., Gakhar, L., Muradov, H., Boyd, K. K., Ramaswamy, S., and Artemyev, N. O. (2009) *EMBO J.* **28,** 3613–3622
6. Kameni Tcheudji, J. F., Lebeau, L., Virmaux, N., Maftei, C. G., Cote, R. H., Lugnier, C., and Schultz, P. (2001) *J. Mol. Biol.* **310,** 781–791
7. Zhang, X. J., Cahill, K. B., Elfenbein, A., Arshavsky, V. Y., and Cote, R. H. (2008) *J. Biol. Chem.* **283,** 29699–29705
8. Song, J., Guo, L. W., Muradov, H., Artemyev, N. O., Ruoho, A. E., and Markley, J. L. (2008) *Proc. Natl. Acad. Sci. U.S.A.* **105,** 1505–1510
9. Guo, L. W., and Ruoho, A. E. (2008) *Curr. Protein Pept. Sci.* **9,** 611–625
10. Skiba, N. P., Artemyev, N. O., and Hamm, H. E. (1995) *J. Biol. Chem.* **270,** 13210–13215
11. Granovsky, A. E., and Artemyev, N. O. (2001) *Biochemistry* **40,** 13209–13215
12. Artemyev, N. O., Natochin, M., Busman, M., Schey, K. L., and Hamm, H. E. (1996) *Proc. Natl. Acad. Sci. U.S.A.* **93,** 5407–5412
13. Granovsky, A. E., Natochin, M., and Artemyev, N. O. (1997) *J. Biol. Chem.* **272,** 11686–11689
14. Mou, H., and Cote, R. H. (2001) *J. Biol. Chem.* **276,** 27527–27534
15. Muradov, K. G., Granovsky, A. E., Schey, K. L., and Artemyev, N. O. (2002) *Biochemistry* **41,** 3884–3890
16. Guo, L. W., Muradov, H., Hajipour, A. R., Sievert, M. K., Artemyev, N. O., and Ruoho, A. E. (2006) *J. Biol. Chem.* **281,** 15412–15422
17. Artemyev, N. O., Rarick, H. M., Mills, J. S., Skiba, N. P., and Hamm, H. E. (1992) *J. Biol. Chem.* **267,** 25067–25072
18. Skiba, N. P., Bae, H., and Hamm, H. E. (1996) *J. Biol. Chem.* **271,** 413–424
19. Granovsky, A. E., McEntaffer, R., and Artemyev, N. O. (1998) *Cell Biochem. Biophys.* **28,** 115–133
20. Slep, K. C., Kercher, M. A., He, W., Cowan, C. W., Wensel, T. G., and Sigler, P. B. (2001) *Nature* **409,** 1071–1077
21. Cheever, M. L., Snyder, J. T., Gershburg, S., Siderovski, D. P., Harden, T. K., and Sondek, J. (2008) *Nat. Struct. Mol. Biol.* **15,** 155–162
22. Navon, S. E., and Fung, B. K. (1988) *J. Biol. Chem.* **263,** 489–496
23. Catty, P., Pfister, C., Bruckert, F., and Deterre, P. (1992) *J. Biol. Chem.* **267,**

19489–19493
24. Clerc, A., and Bennett, N. (1992) *J. Biol. Chem.* **267,** 6620–6627
25. Tsang, S. H., Woodruff, M. L., Chen, C. K., Yamashita, C. Y., Cilluffo, M. C., Rao, A. L., Farber, D. B., and Fain, G. L. (2006) *J. Neurosci.* **26,** 4472–4480
26. Norton, A. W., D'Amours, M. R., Grazio, H. J., Hebert, T. L., and Cote, R. H. (2000) *J. Biol. Chem.* **275,** 38611–38619
27. Clerc, A., Catty, P., and Bennett, N. (1992) *J. Biol. Chem.* **267,** 19948–19953
28. Guo, L. W., Grant, J. E., Hajipour, A. R., Muradov, H., Arbabian, M., Artemyev, N. O., and Ruoho, A. E. (2005) *J. Biol. Chem.* **280,** 12585–12592
29. Grant, J. E., Guo, L. W., Vestling, M. M., Martemyanov, K. A., Arshavsky, V. Y., and Ruoho, A. E. (2006) *J. Biol. Chem.* **281,** 6194–6202
30. Liu, Y., Arshavsky, V. Y., and Ruoho, A. E. (1996) *J. Biol. Chem.* **271,** 26900–26907
31. Guo, L. W., Assadi-Porter, F. M., Grant, J. E., Wu, H., Markley, J. L., and Ruoho, A. E. (2007) *Protein Expr. Purif.* **51,** 187–197
32. Martemyanov, K. A., and Arshavsky, V. Y. (2002) *J. Biol. Chem.* **277,** 32843–32848
33. Baehr, W., Devlin, M. J., and Applebury, M. L. (1979) *J. Biol. Chem.* **254,** 11669–11677
34. Slepak, V. Z., Artemyev, N. O., Zhu, Y., Dumke, C. L., Sabacan, L., Sondek, J., Hamm, H. E., Bownds, M. D., and Arshavsky, V. Y. (1995) *J. Biol. Chem.* **270,** 14319–14324
35. Tanaka, Y., Bond, M. R., and Kohler, J. J. (2008) *Mol. Biosyst.* **4,** 473–480
36. Noel, J. P., Hamm, H. E., and Sigler, P. B. (1993) *Nature* **366,** 654–663
37. Artemyev, N. O., and Hamm, H. E. (1992) *Biochem. J.* **283,** 273–279
38. Artemyev, N. O., Mills, J. S., Thornburg, K. R., Knapp, D. R., Schey, K. L., and Hamm, H. E. (1993) *J. Biol. Chem.* **268,** 23611–23615
39. Brown, R. L. (1992) *Biochemistry* **31,** 5918–5925
40. Melia, T. J., Malinski, J. A., He, F., and Wensel, T. G. (2000) *J. Biol. Chem.* **275,** 3535–3542
41. Nair, K. S., Balasubramanian, N., and Slepak, V. Z. (2002) *Curr. Biol.* **12,** 421–425
42. Kerov, V., Rubin, W. W., Natochin, M., Melling, N. A., Burns, M. E., and Artemyev, N. O. (2007) *J. Neurosci.* **27,** 10270–10277
43. Arshavsky, V. Y., Dumke, C. L., and Bownds, M. D. (1992) *J. Biol. Chem.* **267,** 24501–24507
44. Cote, R. H., Bownds, M. D., and Arshavsky, V. Y. (1994) *Proc. Natl. Acad. Sci. U.S.A.* **91,** 4845–4849
45. Krispel, C. M., Chen, D., Melling, N., Chen, Y. J., Martemyanov, K. A., Quillinan, N., Arshavsky, V. Y., Wensel, T. G., Chen, C. K., and Burns, M. E. (2006) *Neuron* **51,** 409–416
46. Liu, Y. T., Matte, S. L., Corbin, J. D., Francis, S. H., and Cote, R. H. (2009) *J. Biol. Chem.* **284,** 31541–31547